Paper C

Dimensionless Time Traces of Mechanical Dynamics in Papillary Muscle Twitches

Vidar Sørhus[1], Marc J. Demolder[2], Stein I. Rabben[1], Bjørn A. J. Angelsen[1], and Stanislas U. Sys[2]

[1] Dept. of Physiology and Biomedical Engineering, NTNU, Trondheim, Norway

[2] Dept. of Human Physiology and Pathophysiology, UIA (RUCA), Antwerp, Belgium

Abstract

The mechanical dynamics of cardiac muscles are expressed as changes in muscle length and force. In isolated muscle, the length and force dynamics have been studied separately. Under auxotonic loading conditions, however, there are simultaneous changes in length and force. We wanted to study the differences in mechanical dynamics in twitches with different loading conditions. We represented the mechanical dynamics with two different expressions, defined as the sum of normalized stress and shortening. The first used normalized developed stress and the second used normalized instantaneous active stress as input. The resulting dimensionless time traces of mechanical dynamics demonstrated very similar shape of the contraction phase at the full range of loads from isotonic to isometric and in both auxotonic and afterloaded twitches. The same traces demonstrated wide variation during relaxation depending on load and twitch type. With the first expression, it was possible to obtain a rough estimate of peak isometric stress and peak isotonic shortening from two or more intermediate twitches. Both expressions visualized qualitative differences in load dependence between the contraction and relaxation phases, which may have implications on the clinical interpretation of systolic versus diastolic function.

Keywords: load dependence; cardiac muscle; auxotonic; contraction-relaxation; systolic function; diastolic function

1 Introduction

Mechanical dynamics in cardiac muscles can be defined as changes in muscle length and force. The changes in length and force result from interactions between force-generating units (cross-bridges) in the muscle and the loading conditions applied on the muscle. Shortening occurs when the force generated by the cross-bridges exceeds the load on the cross-bridges. Instantaneous force is given by the number of cross-bridges and the mean force on each cross-bridge, which in turn depend on loading conditions, calcium handling, and properties of the contractile proteins [9].

The mechanical dynamics of the fully activated (tetanized) muscle have been studied from quick release (and quick stretch) experiments, constant velocity experiments, and sinusoidal perturbation [10, 13, 19, 20, 23]. These experiments have been used to obtain information about the cross-bridge dynamics. The cross-bridge dynamics have been represented by the force-velocity relation with the related Hill equation and force recovery time constants [14, 20, 23].

In traditional experimental setups for isolated papillary muscles, the muscle twitches (single contraction-relaxation sequences) have been controlled in either isometric (constant length) or isotonic (constant total force) conditions or sequential combinations of isometric and isotonic loading conditions [9, 26, 28]. In muscle twitches, the sarcomeres are not fully activated. In such twitches we observe an initial transient rise in activation which is continued with a relaxation phase. This means that the mechanical dynamics result from a combination of activation dynamics and cross-bridge dynamics. It is not well-known whether the cross-bridge dynamics is the same under sub-maximal activation as it is under maximal activation and thereby separable from the activation dynamics.

The mechanical dynamics of muscle twitches have been quantified with indices like (positive and negative) peak dF/dt and peak shortening and peak lengthening velocity [4, 24]. These indices are related to intact heart measures like peak positive and negative dP/dt and maximal velocities of ejection and filling flow [3, 4]. The slope of the last part of the isovolumetric pressure decline has been used as an index of impaired relaxation or diastolic function [22].

In the intact heart, there are coupled and simultaneous changes in both length and stress during all phases of the cardiac cycle [7, 12, 15, 17, 29, 30]. Changes in length and stress are coupled both through the loading conditions and their common origin, namely the cross-bridge cycling. Therefore, mechanical dynamics are expressed as changes in both stress and length, more or less simultaneously. Single measures of mechanical dynamics based on either stress or shortening may therefore be dependent on the loading conditions and insufficient to describe the true mechanical dynamics. To be able to study isolated muscles with simultaneous changes in length and stress, we included auxotonic loading in an experimental setup for isolated papillary muscles [33].

The purpose of this study was to compare the mechanical dynamics of isolated papillary muscles under different loading conditions. We therefore constructed two different expressions of the mechanical dynamics, defined as the sum of normalized stress and shortening. Based on these expressions we wanted to 1) visualize the qualitative differences in mechanical dynamics between twitches with different loading conditions, 2) derive quantitative parameters of the muscle performance, and 3) discuss the influence of the loading conditions on cardiac muscle modeling.

2 Methods

2.1 Muscle Preparation

Rabbits (n=9) were anesthetized by cervical translocation and the heart was quickly excised. A papillary muscle was dissected from the right ventricle in a dissection bath with temperature controlled and oxygenated Krebs-Ringer solution (see below), containing 2,3-butanedione monoxime (BDM; 30mM) to inhibit actin-myosin cross-bridge cycling during dissection. The muscle was passively stretched with a preload of 6 mN/mm^2 of estimated cross-sectional area. Under a dissection microscope (WILD M3B from Leica) three tips of glass microelectrodes were inserted into the muscle perpendicular to the long axis. At the tip, the diameters of the microelectrodes were less than 5 μm, and at the muscle surface the diameters were maximally 15 μm. Then the papillary muscle was installed vertically in a 3 ml bath. The Krebs-Ringer solution was circulating with a flow rate of approximately 10 ml/min and contained (in mM): NaCl 98, KCl 4.7, $MgSO_4.7H_2O$ 2.4, $NaHCO_3$ 25, $CaCl_2.2H_2O$ 1.25, glucose 4.5, Na-pyruvate 15 and Na-acetate 5, at 29°C bubbled with a gas mixture of 95 % oxygen and 5 % carbon dioxide. An electrical field between two platinum electrodes stimulated the papillary muscle at approximately 10 % above threshold.

2.2 Experimental Setup

The papillary muscle setup was based on an analog/mechanical setup, described in Brutsaert and Claes [6] and Brutsaert et al. [8]. The original system consisted of a force transducer, an optical displacement measurement transducer, a papillary muscle bath with a clip for the lower muscle end, two platinum electrodes for electrical stimulation, and a control unit for isotonic and isometric control and stimulation. The system also included a segment measurement system based on detection of position of microelectrodes with a CCD-array [7, 34].

The control unit of the original setup was replaced with a PC with a DSP board and an interface unit between the PC and the transducers, as described in Sørhus et al. [33] (Figure 1). An individual application for low-level feedback control and data acquisition was running on the DSP board at a sample rate of 5000 samples per second. This application included different algorithms for different twitch types.

Another application for visualization and storage of measured and calculated variables, on-line user interaction, and overall control of experiments was running on the host computer.

The system included a controlled auxotonic twitch where the muscle was acting against an virtual ideal spring:

$$\sigma_t(t) \quad = \quad k_a(l_{max} - l(t)) + \sigma_r(l_{max})$$

where σ_t, l, and $\sigma_r(l_{max})$ denote total stress, measured length, and resting stress at the length with maximal isometric active stress development, respectively. The stiffness of the virtual spring was given by the user-defined spring constant, k_a (mN/mm), representing a smooth transition from isotonic ($k_a = 0$) to isometric ($k_a \to \infty$).

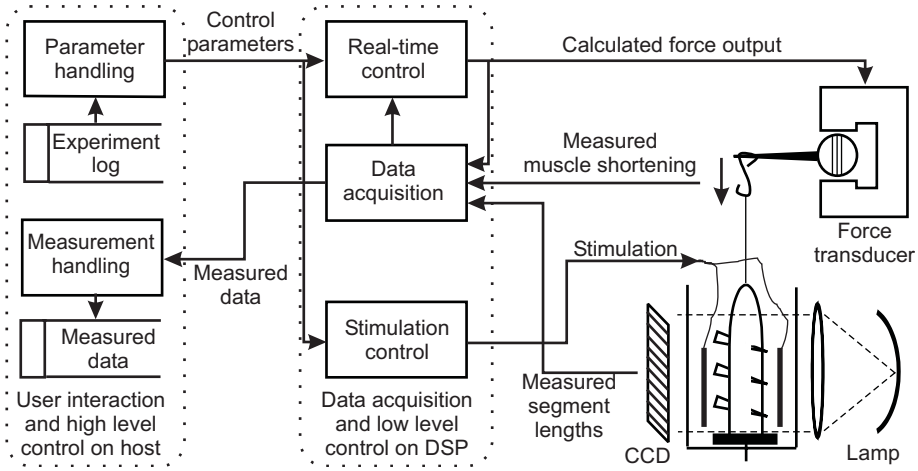

Figure 1: Main components and data flow in the system. An application for real-time control, data acquisition, and stimulation control was running on the DSP board. Total muscle shortening and muscle segment lengths were measured and sent via the DSP-board to the host computer through a measurement channel and optionally stored in a text-file (Measured data). An application for user interaction and high level control was running on the host computer. Control parameters set by the user or read from a text-file (Experiment log) were sent from the host computer to the DSP-board through a parameter channel.

2.3 Dimensionless Expressions of Mechanical Dynamics

To study the mechanical dynamics in twitches including changes in both length and stress, we used two dimensionless expressions, defined as the sum of normalized stress and shortening. We required that the peak value of the expressions in the extreme cases of isotonic and isometric twitches should be normalized (= 1). In the first expression we used only total stress and muscle shortening:

$$M1(t) = \frac{\sigma_t(t) - \sigma_r(l_{max})}{max\{\sigma_{a,im}\}} + \frac{\varepsilon(t)}{max\{\varepsilon_{it}\}} \quad (1)$$

where

$$\begin{aligned} \sigma_a(t) &= \sigma_t(t) - \sigma_r(l(t)) \\ \varepsilon(t) &= 1 - \frac{l(t)}{l_{max}} \end{aligned}$$

σ_t and σ_a denote total and active stress, $\sigma_r(l)$ is resting stress at a given muscle length l, $max\{\sigma_{a,im}\}$ is peak isometric active stress, and $max\{\varepsilon_{it}\}$ is peak isotonic shortening.

Total stress in Eq. 1 is the sum of active and passive stress. One possible shortcoming of expression $M1$ (Eq. 1) is that total stress is constant during isotonic shortening, although active and passive stress changes due to the passive stress-length relation (Figure 2).

An alternative to Eq. 1 is therefore to use active stress instead of developed stress ($\sigma_d = \sigma_t - \sigma_r(l_{max})$). Peak active stress in isotonic twitches is equal to passive stress at l_{max} minus passive stress at the shortest length. Therefore, to obtain equal peak values in the resulting traces of isometric and isotonic twitches, we modified Eq. 1:

$$M2(t) = \frac{\sigma_a(t)}{max\{\sigma_{a,im}\}} + \frac{\varepsilon(t)}{max\{\varepsilon_{it}\}} \cdot \left[1 - \frac{max\{\sigma_{a,it}\}}{max\{\sigma_{a,im}\}}\right] \quad (2)$$

2.4 Experiment Protocol

In nine papillary muscles, we measured one series of afterloaded and one series of physiological twitches with increasing afterload from isotonic to isometric, and one series of auxotonic twitches at different loads from isotonic to isometric. Initial length was l_{max} in all these twitches. Eight isotonic stabilization twitches preceded each measured twitch. One additional series of isometric twitches at increasing length was measured to derive passive stress-length relations for each muscle (Figure 2).

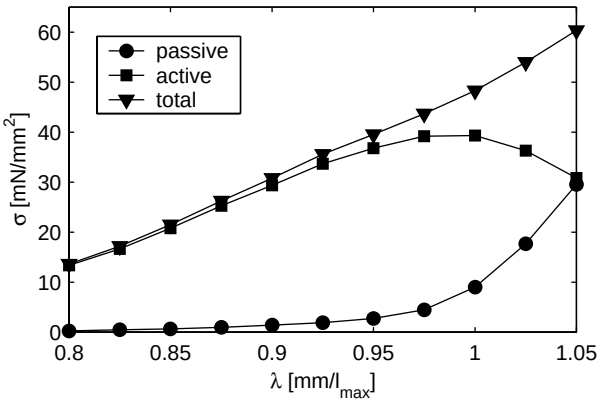

Figure 2: Passive (circles), active (squares), and total (triangles) stress-length relations from a series of isometric twitches at increasing length.

2.5 Data Analysis

We used Eq. 1 and 2 to calculate time traces of dimensionless mechanical dynamics ($M1$ and $M2$) for all muscles and all twitches. The individual passive stress-length relations were used to calculate instantaneous active stress in afterloaded, physiological, and auxotonic twitches. We measured resting diameter of all muscles at l_{max} to calculate cross-sectional area. We have used stress (force per resting cross sectional area) and relative length ($\lambda = l/l_{max}$) in all analyses where nothing else is noticed.

Expression $M1$ was used to estimate peak isometric stress and peak isotonic shortening with two different methods. First, we used linear regression on all the intermediate twitches. In this case, the peak values were calculated according to

$$\alpha = (A^T A)^{-1} A^T y \tag{3}$$

where

$$\begin{aligned} \alpha &= [1/max\{\sigma_{a,im}\} \quad 1/max\{\varepsilon_{it}\}]^T \\ A &= \begin{bmatrix} max\{\sigma_d, tw1\} & max\{\varepsilon, tw1\} \\ \vdots & \vdots \\ max\{\sigma_d, twN\} & max\{\varepsilon, twN\} \end{bmatrix} \\ y &= [1 \cdots 1]^T \qquad \text{or} \qquad y = [0.94 \cdots 0.94]^T \end{aligned}$$

Second, we calculated peak isometric stress and peak isotonic shortening from all pairs of intermediately loaded twitches. For both methods we used both the peak value of the isometric and isotonic twitches (= 1) and the average peak value of the intermediate twitches (= 0.94, see Results) as the intercept (y in Eq. 3).

The calculation and visualization of $M1$ and $M2$ and the estimation of peak isometric stress and peak isotonic shortening were performed with Matlab (MathWorks Inc.). All statistical analysis were performed with Excel (Microsoft Corp.).

3 Results

3.1 Dimensionless Time Traces of Mechanical Dynamics

Figure 3 presents time traces of total stress (panel A), relative length (panel B), and mechanical dynamics from the two expressions $M1$ (Eq. 1, panel C) and $M2$ (Eq. 2, panel D) from a series of afterloaded twitches with increasing afterload from isotonic to isometric. Figure 4 and 5 demonstrate similar plots of a series of physiological (i.e. isometric-isotonic relaxation sequence) twitches at increasing afterload and a series of auxotonic twitches at increasing auxotonic load from the same muscle. All series of twitches included one isotonic and one isometric reference twitch.

3.1.1 Contraction

An interesting observation about the mechanical dynamics in the contraction phase was that $M1$ and $M2$ varied little at different loading conditions and twitch types. There was a small reduction in the rate of mechanical dynamics after an abrupt change from isometric to isotonic contraction when expression $M1$ was used. In the other expression ($M2$), when active stress was used instead of total stress, there was very little difference between twitches with different loading. The same small variation in mechanical dynamics during contraction was found when we performed a series of twitches with a non-physiological isotonic-isometric contraction sequence (Figure 8).

3.1.2 Relaxation

During relaxation dynamics, however, $M1$ and $M2$ demonstrated considerable differences in mechanical dynamics dependent on the loading conditions. The difference between isotonic and isometric rate of $M1$ and $M2$ during relaxation was clearly demonstrated in the physiological twitches (Figure 4), where we had an isometric-isotonic relaxation sequence. Mechanical dynamics during isotonic relaxation were markedly faster than during isometric relaxation. Time from stimulus did not seem to change the rates of $M1$ and $M2$ markedly. The same may also be true for the afterloaded twitches (Figure 3), although the transition from isotonic to isometric relaxation yielded a very fast initial isometric stress decline.

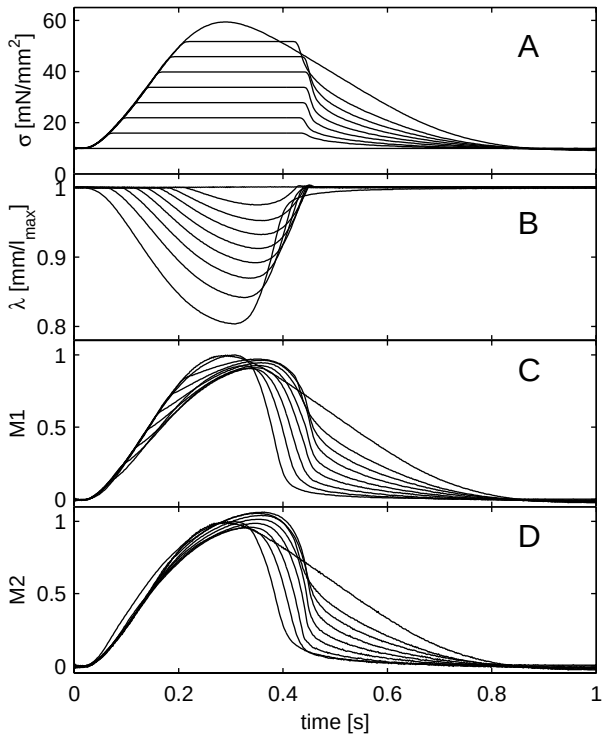

Figure 3: Total stress (A), relative length (B), $M1$ (C), and $M2$ (D) from a series of afterloaded twitches at increasing afterload from isotonic to isometric.

In both the afterloaded and the physiological twitches, there were abrupt changes between isotonic and isometric loading conditions. After these abrupt changes, there seemed to be a small transition time before the mechanical dynamics followed the expected isotonic or isometric patterns. In afterloaded relaxation, the change was from fast (isotonic) to slow (isometric), and therefore the initial stress decline was fast.

So far, we have noticed the fast isotonic and the slow isometric rate of relaxation. The auxotonic twitches were supposed to give a smooth transition from isotonic to isometric loading. The rate of relaxation in the auxotonic twitches (Figure 5), in terms of the two dimensionless expressions defined here, seemed to give a similar smooth transition in the rate of relaxation; from isotonic towards isometric at increasing auxotonic load (k_a). We observed a decreasing rate of relaxation when k_a increased from isotonic towards isometric.

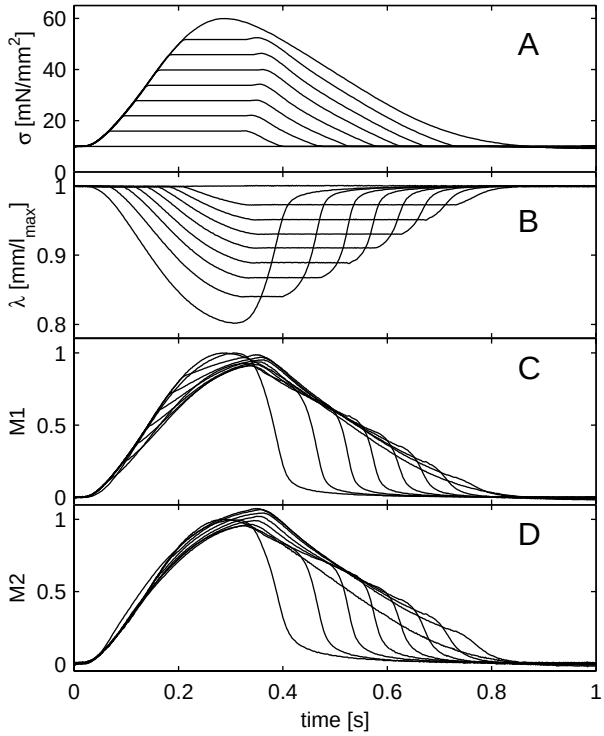

Figure 4: Total stress (A), relative length (B), $M1$ (C), and $M2$ (D) from a series of physiological twitches at increasing afterload from isotonic to isometric.

3.2 Peak Values of Intermediately Loaded Twitches

One requirement for the dimensionless expression of the mechanical dynamics was that the peak value of the time trace should be equal for isotonic and isometric twitches. In the examples in Figure 3 to 5, the peak values of the intermediately loaded twitches were also close to the peak values of the isotonic and isometric twitches ($max\{M1\} = max\{M2\} = 1$).

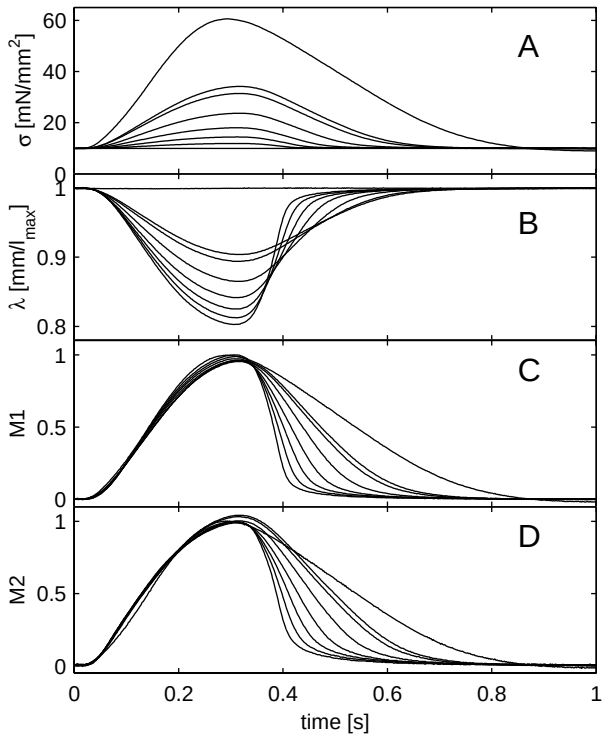

Figure 5: Total stress (A), relative length (B), $M1$ (C), and $M2$ (D) from a series of auxotonic twitches at increasing auxotonic load from isotonic to isometric.

Table 1 presents the average peak values of the intermediate twitches (all twitches except isotonic and isometric) of all twitch types and for both dimensionless expressions ($M1$ and $M2$). For $M1$, the peak values were less than 1, and in general lower for afterloaded and physiological twitches than for auxotonic twitches (paired t-test; $P<0.0001$). This may be related to the discontinuities in the stress and length due to the abrupt change between isometric and isotonic loading conditions [33]. When we used instantaneous active stress in the dimensionless expression ($M2$), we obtained peak values close to one in all twitch types. The more equal peak values of $M2$ in afterloaded and physiological twitches compared to auxotonic twitches, are partly due to the different distribution of twitches between isotonic and isometric and to the non-linear passive stress-length relation (Figure 2).

Table 1: Peak values of $M1$ and $M2$ in all twitches except isotonic and isometric twitches (n=9).

	Afterloaded	Physiological	Auxotonic	All
$max\{M1(t)\}$ (mean ± SD)	0.931 ± 0.031	0.937 ± 0.034	0.961 ± 0.022	0.944 ± 0.032
$max\{M2(t)\}$ (mean ± SD)	1.011 ± 0.035	1.016 ± 0.039	1.011 ± 0.022	1.012 ± 0.032

3.3 Estimation of Peak Isometric Stress and Peak Isotonic Shortening

Based on the fact that the peak values of the intermediately loaded twitches were close to the peak values of the isometric and isotonic twitches, it may be possible to estimate the peak isometric stress and peak isotonic shortening from two or more intermediately loaded twitches. The peak values from the $M2$-expression were closest to one. This expression, however, required that the passive stress-length relation was known from isometric measurements, and therefore estimation of peak isometric stress was not interesting. Expression $M1$ only requires total stress and shortening from at least two differently loaded twitches as input. Therefore, we used this expression to estimate peak isometric stress and peak isotonic shortening. We used two different methods as described in the Methods section. First, we used linear regression on all the intermediate twitches (Eq. 3). Second, we calculated peak isometric stress and peak isotonic shortening from all pairs of intermediately loaded twitches. The resulting estimation errors from the two methods are presented as bar-plots in Figure 6 and 7.

As one would expect from the peak values in Table 1, we got a small underestimation of the peak values with both methods. In auxotonic twitches, the estimation of peak isotonic shortening was better than the estimation of the peak isometric stress. In afterloaded and physiological twitches, the twitches were isometric in the first part of the contraction before they were switched to isotonic. The average estimation error and the variance were a little higher for the second estimation method (all pairs of intermediate twitches).

4 Discussion

This study has presented two possible expressions for the mechanical dynamics of cardiac muscle twitches. Both expressions combine stress and length dynamics. This makes it possible to compare the mechanical dynamics of twitches with different loading conditions from isotonic to isometric. Both expressions demonstrate fundamental differences between the mechanical dynamics in contraction and in relaxation.

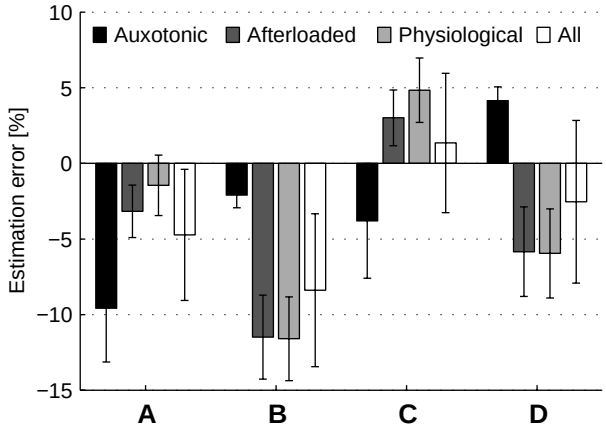

Figure 6: Estimation error (mean ± SD, n= 9) from estimation of peak isometric stress (A and C) and peak isotonic shortening (B and D). Linear regression with one on the intercept in A and B, and linear regression with the average peak value of $M1$ (Table 1) on the intercept in C and D.

4.1 Mechanical Dynamics in Twitches

Mechanical dynamics in the intact heart have traditionally been studied with different measures like positive and negative peak dP/dt, positive and negative peak velocities, and pressure-volume relations. Some of the measures have been normalized in different ways and used as indices on contractility and diastolic function [4, 22]. Similar measures for isolated muscles are peak dF/dt and v_{max}. Such measures may be misleading and not represent the true mechanical dynamics in twitches with sequences of isotonic and isometric phases. For example, in afterloaded twitches (Figure 3) peak dF/dt will increase with increasing afterload level, until the afterload exceeds the force with peak dF/dt in the complete isometric twitch. When normalized to, for instance, peak force, the dependence on the loading condition is even more pronounced [32]. To be able to visualize the qualitative differences in mechanical dynamics in twitches with different loading conditions, we proposed two expressions of the mechanical dynamics as the sum of normalized stress and shortening. Notice, that due to the same series of stabilization twitches before each recorded twitch, the contractile state and metabolic state were the same in all our experiments. Therefore, the differences in the $M1$ and $M2$ traces are all load-dependent differences, and not differences in, for instance, contractility.

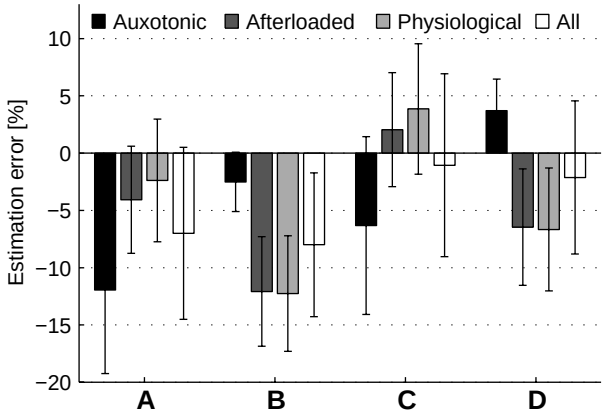

Figure 7: Estimation error (mean ± SD, n= 9) from estimation of peak isometric stress (A and C) and peak isotonic shortening (B and D). Calculated form all pairs of intermediately loaded twitches. Estimates calculated with one on the intercept in A and B, and with the average peak value of $M1$ (Table 1) on the intercept in C and D.

4.2 Mechanical Dynamics during Contraction and Relaxation

When we used the proposed expressions ($M1$ and $M2$) to calculate the mechanical dynamics in twitches with different loading conditions from isotonic to isometric, the most remarkable result was the difference between the contraction and relaxation phases. Even when the contraction phase was separated in one isometric and one isotonic phase, the contraction phase of the $M1$ and $M2$ traces had very similar shape. In relaxation, however, the $M1$ and $M2$ traces were widely separated depending on the loading condition and loading history. The latter demonstrates the concept of load dependence of relaxation [9, 34]. The independence of the amount of shortening and stress development on the contraction phase indicates that the common shape reflects the relative time-course of recruitment of new cross-bridges. In isometric contraction, this only adds force. Araki et al. [2] represent isovolumetric pressure rise with a function of the probability that the inhibitory effect of each single tropomyosin is removed within a given time after stimulation. During shortening, the recruitment of new cross-bridges compensates for the detachment of other cross-bridges and the reduction of the single overlap region in the sarcomere [21].

Activation (contraction) and inactivation (active relaxation) may be balanced by the level of free Ca^{2+} in the cytoplasm. During relaxation, there is a net amount of Ca^{2+} that dissociates from troponin C and enters the cytoplasm, where it is pumped

into the sarcoplasmic reticulum and out of the cell through the cell membrane. It has been reported that force-bearing cross-bridges have a cooperative effect on activation [5, 11, 16, 18, 21, 31]. This may be partly responsible for the difference in rate of relaxation in isotonic and isometric twitches. During isotonic lengthening, the number of cycling cross-bridges must be higher than during isometric force decline at the same force. Given a lower rate of inactivation for sites on the thin filament that are attached to cross-bridges versus sites that are not attached to cross-bridges, the isotonic relaxation will be faster than isometric relaxation.

4.3 Effect of the Transition between Isometric and Isotonic Loading on Mechanical Dynamics

There are four different abrupt changes between the two extreme isotonic and isometric loading conditions in our experiments. These are 1) from isometric to isotonic during contraction (Figure 3 and 4), 2) from isotonic to isometric during contraction (Figure 8), 3) from isotonic to isometric during relaxation (Figure 3), and 4) from isometric to isotonic during relaxation (Figure 4 and 8).

Not only the change in the number of cross-bridges determine the changes in active stress. During shortening and lengthening, some cross-bridges will either be moved from the single overlap region into the double overlap region (shortening) or in the opposite direction (lengthening) [21]. This effect may be observed after abrupt changes from isometric to isotonic or from isotonic to isometric loading. Other factors may also be partly responsible for the observed transition in the dynamics after switches between isometric and isotonic conditions. Viscous effects of muscle fibers and the surrounding tissue may play a role as well as transition from kinetic to potential energy which may be responsible for additional break-down of cross-bridges (in afterloaded twitches). Brutsaert and Sys [9] explain the rapid initial force decline in afterloaded twitches as an inherent property of the preceding lengthening process.

4.4 Estimation of Muscle Performance Parameters

Like in time traces of stress and length, it is possible to extract peak values and timing parameters from the $M1$ and $M2$ traces. In afterloaded and physiological twitches with sequences of isometric and isotonic loading conditions, it is not possible to measure time to half contraction and time to half relaxation from individual stress and length traces. This, however, is possible from the $M1$ and $M2$ traces.

We found that the $M1$ expression could also be used to obtain estimates of the peak isometric stress and peak isotonic shortening from intermediately loaded twitches. In auxotonic twitches, the estimation of peak isotonic shortening was better than the estimation of the peak isometric stress. This may be due to more auxotonic twitches closer to isotonic than to isometric loading. In afterloaded and physiological twitches, the twitches were isometric in the first part of the contraction before they abruptly

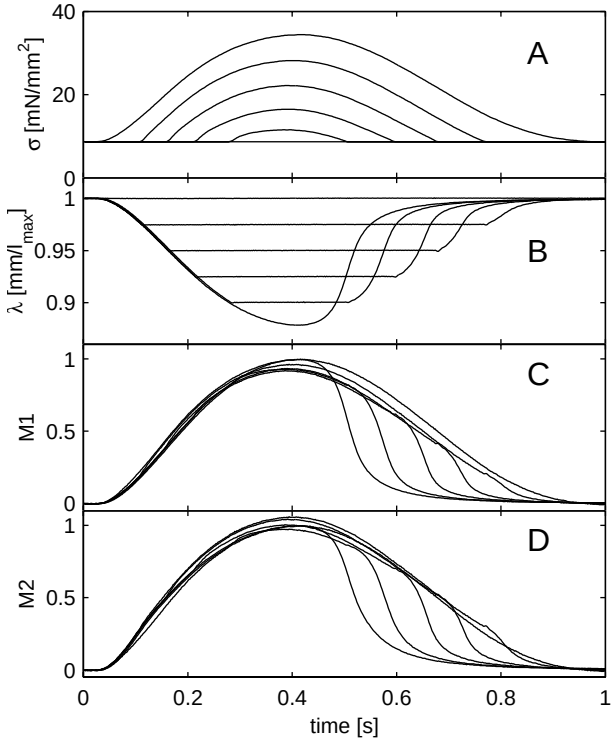

Figure 8: Total stress (A), relative length (B), $M1$ (C), and $M2$ (D) from a series of twitches with isotonic-isometric contraction sequence and isometric-isotonic relaxation sequence at decreasing peak shortening from isotonic to isometric.

changed to isotonic. This may be the reason why these twitches had the best estimates of peak isometric stress.

The average estimation error and the variance were a little higher for the second estimation method (all pairs of intermediate twitches). With this method, some pairs were close to each other and at the same time close to either isotonic or isometric loading. In such cases, the estimation of the other extreme loading may be difficult. We made no attempt to exclude such cases.

4.5 Consequences for Cardiac Muscle Modeling

It is difficult to develop mathematical models of the cardiac muscle that incorporates the differences in load dependence of contraction and relaxation and the many, more or less coupled, underlying processes. Especially if one wants to simulate muscle twitches over a wide range of loading conditions. A number of investigators use a compartment approach in the modeling of the cardiac muscle function [21, 27, 31]. This model approach is especially suitable for modeling the calcium and thin filament activation. This way it may be possible to incorporate cooperativity and length-dependent activation related to calcium sensitivity [1]. One of the fundamental problems with this model-approach is that it is to a high degree based on results from isometric and to some degree calcium-activated experiments. It may, therefore, be a challenge to extrapolate these models also to simulate non-isometric behavior adequately.

In a much more phenomenological approach, Araki and co-workers [2, 22, 25] has fitted the isovolumetric pressure curve and isometric force curve to a combination of two logistic functions. The problem with this approach is that it only represents isometric (and isovolumetric) conditions. The first function, representing the contraction phase, should also fit to the contraction phase of the traces from our dimensionless expressions because these traces are very similar to the isometric force trace. This implies that the logistic function of contraction may also represent non-isometric conditions or sequences of isotonic and isometric conditions. It is also reasonable that it is possible to fit the second function to the relaxation phase of the dimensionless expressions for all the auxotonic twitches from isotonic to isometric. For the afterloaded and physiological twitches, however, there will be a transition between the slopes of two different logistic functions representing the isotonic and isometric relaxation. This is again due to the concept of load dependence of relaxation [9].

The results presented in this paper demonstrate a coupling between changes in stress and changes in length in cardiac muscle twitches at a wide range of loading conditions. Quantitatively, for example as the relation between the peak isometric stress development and peak isotonic shortening and the peak values of the intermediately loaded twitches. Qualitatively, for example as the differences in rate of lengthening and rate of stress decline. Such relations may be used as constraints on cardiac muscle models.

4.6 Clinical Relevance

In a clinical setting, it is very important to distinguish between observations that result from altered muscle properties and observations that result from altered loading conditions [3]. Therefore, it has been focused on how to extract load-independent indices of contractility from different measurements [4]. We have demonstrated that for the whole range of afterloaded and auxotonic loading conditions from isotonic to isometric, the sum of the normalized stress and shortening is nearly load-independent during contraction. But, even though the pattern of the contraction phase is barely

load dependent, the distribution of stress versus shortening has major implications on the patterns of the relaxation phase.

This study shows that more stress development during contraction leads to a prolonged relaxation. Therefore, what may be interpreted as an impaired relaxation due to a prolonged isovolumetric relaxation time (or rate), may in fact be a result of increased systolic stress development due to pressure or volume overload.

4.7 Conclusions

This study has presented two possible expressions for the mechanical dynamics of cardiac muscle twitches. Both expressions combine stress and length dynamics. This makes it possible to compare the mechanical dynamics of twitches with different loading conditions from isotonic to isometric. The $M2$ expression had peak values close to one for all twitch types and loading conditions, and $M2$ may therefore better demonstrate the active dynamics of the muscle. However, with the $M1$ expression it is possible to obtain a rough estimate of peak isometric stress and peak isotonic shortening form measurements of total stress and shortening. Both expressions demonstrate fundamental differences between contraction and relaxation dynamics.

Acknowledgements: This research has been supported in part by the Norwegian Research Council (NFR) grant # 107409/320.

References

1. Allen DG and Kentish JC. The cellular basis of the length-tension relation in cardiac muscle. *J. Mol. Cell. Cardiol.* 17:821–40, 1985. 4.5

2. Araki J, Matsubara H, Shimizu J, Mikane T, Mohri S, Mizuno J, Takaki M, Ohe T, Hirakawa M, and Suga H. Weibull distribution function for cardiac contraction: Integrative analysis. *Am. J. Physiol.* 277:H1940–H1945, 1999. 4.2, 4.5

3. Borow KM, Neumann A, Marcus RH, Sareli P, and Lang RM. Effects of simultaneous alterations in preload and afterload on measurements of left ventricular contractility in patients with dilated cardiomyopathy: Comparisons of ejection phase, isovolumetric and end- systolic force-velocity indexes. *J. Am. Coll. Cardiol.* 20:787–95, 1992. 1, 4.6

4. Braunwald E. Assessment of cardiac function. In: Braunwald E, ed., *Heart Disease: A Textbook of Cardiovascular Medicine*, volume 1, 419–443. W. B. Saunders Company, Philadelphia, USA, 4th edition, 1992. 1, 1, 4.1, 4.6

5. Bremel RD and Weber A. Cooperation within actin filament in vertebrate skeletal muscle. *Nat. New. Biol.* 238:97–101, 1972. 4.2

6. Brutsaert DL and Claes VA. Onset of mechanical activation of mammalian heart muscle in calcium- and strontium-containing solutions. *Circ. Res.* 35:345–57, 1974. 2.2

7. Brutsaert DL, Claes VA, Chuck LM, Housmans PR, Sys SU, and DeClerck NM. New technology in studying the origin of non-uniformity in cardiac muscle. In: Kitamura K and Abe H, eds., *New approaches in cardiac mechanics*, 31–45. Gordon and Breach, New York, USA, 1986. 1, 2.2

8. Brutsaert DL, Meulemans AL, Sipido KR, and Sys SU. Effects of damaging the endocardial surface on the mechanical performance of isolated cardiac muscle. *Circ. Res.* 62:358–66, 1988. 2.2

9. Brutsaert DL and Sys SU. Relaxation and diastole of the heart. *Physiol. Rev.* 69:1228–315, 1989. 1, 1, 4.2, 4.3, 4.5

10. de Tombe PP and ter Keurs HE. Sarcomere dynamics in cat cardiac trabeculae. *Circ. Res.* 68:588–96, 1991. 1

11. Fitzsimons DP and Moss RL. Strong binding of myosin modulates length-dependent Ca2+ activation of rat ventricular myocytes. *Circ. Res.* 83:602–7, 1998. 4.2

12. Gibbons Kroeker CA, Ter Keurs HE, Knudtson ML, Tyberg JV, and Beyar R. An optical device to measure the dynamics of apex rotation of the left ventricle. *Am. J. Physiol.* 265:H1444–9, 1993. 1

13. Hancock WO, Martyn DA, and Huntsman LL. Ca2+ and segment length dependence of isometric force kinetics in intact ferret cardiac muscle. *Circ. Res.* 73:603–11, 1993. 1

14. Hill AV. The heat of shortening and the dynamic constants of muscle. *Proc. R. Soc. Ser. B* 126:136–195, 1938. 1

15. Hittinger L, Crozatier B, Belot JP, and Pierrot M. Regional ventricular segmental dynamics in normal conscious dogs. *Am. J. Physiol.* 253:H713–9, 1987. 1

16. Hofmann PA and Fuchs F. Evidence for a force-dependent component of calcium binding to cardiac troponin C. *Am. J. Physiol.* 253:C541–6, 1987. 4.2

17. Housmans PR, Chuck LH, Claes VA, and Brutsaert DL. Nonuniformity of contraction and relaxation of mammalian cardiac muscle. *Adv. Exp. Med. Biol.* 170:837–40, 1984. 1

18. Housmans PR, Lee NK, and Blinks JR. Active shortening retards the decline of the intracellular calcium transient in mammalian heart muscle. *Science* 221:159–61, 1983. 4.2

19. Hunter PJ, McCulloch AD, and ter Keurs HE. Modelling the mechanical properties of cardiac muscle. *Prog. Biophys. Mol. Biol.* 69:289–331, 1998. 1

20. Huxley AF and Simmons RM. Proposed mechanism of force generation in striated muscle. *Nature* 233:533–8, 1971. 1, 1

21. Landesberg A and Sideman S. Mechanical regulation of cardiac muscle by coupling calcium kinetics with cross-bridge cycling: A dynamic model. *Am. J. Physiol.* 267:H779–95, 1994. 4.2, 4.2, 4.3, 4.5

22. Matsubara H, Takaki M, Yasuhara S, Araki J, and Suga H. Logistic time constant of isovolumic relaxation pressure-time curve in the canine left ventricle. Better alternative to exponential time constant. *Circulation* 92:2318–26, 1995. 1, 4.1, 4.5

23. McMahon TA. *Muscles, Reflexes, and Locomotion*. Princeton University Press, Princeton, New Jersey, USA, 1984. 1, 1

24. Milnor WR. *Hemodynamics*. Williams & Wilkins, Baltimore, USA, 2nd edition, 1989. 1

25. Mizuno J, Mikane T, Araki J, Hatashima M, Moritan T, Ishikawa T, Komukai K, Kurihara S, Hirakawa M, and Suga H. Hybrid logistic characterization of isometric twitch force curve of isolated ferret right ventricular papillary muscle. *Jpn. J. Physiol.* 49:145–58, 1999. 4.5

26. Peterson JN, Hunter WC, and Berman MR. Control of segment length or force in isolated papillary muscle: An adaptive approach. *Am. J. Physiol.* 256:H1726–34, 1989. 1

27. Peterson JN, Hunter WC, and Berman MR. Estimated time course of Ca2+ bound to troponin C during relaxation in isolated cardiac muscle. *Am. J. Physiol.* 260:H1013–24, 1991. 4.5

28. Pinto JG. A constitutive description of contracting papillary muscle and its implications to the dynamics of the intact heart. *J. Biomech. Eng.* 109:181–91, 1987. 1

29. Rademakers FE, Buchalter MB, Rogers WJ, Zerhouni EA, Weisfeldt ML, Weiss JL, and Shapiro EP. Dissociation between left ventricular untwisting and filling. Accentuation by catecholamines. *Circulation* 85:1572–81, 1992. 1

30. Rayhill SC, Daughters GT, Castro LJ, Niczyporuk MA, Moon MR, Ingels NBJ, Stadius ML, Derby GC, Bolger AF, and Miller DC. Dynamics of normal and ischemic canine papillary muscles. *Circ. Res.* 74:1179–87, 1994. 1

31. Rice JJ, Winslow RL, and Hunter WC. Comparison of putative cooperative mechanisms in cardiac muscle: Length dependence and dynamic responses. *Am. J. Physiol.* 276:H1734–54, 1999. 4.2, 4.5

32. Sørhus V, Angelsen BAJ, and Sys SU. Analysis of the controlled auxotonic twitch in isolated cardiac muscle. *Submitted* 2000. 4.1

33. Sørhus V, Sys SU, Natås A, Demolder MJ, and Angelsen BAJ. Controlled auxotonic twitch in papillary muscle: A new computer-based control approach. *Submitted* 2000. 1, 2.2, 3.2

34. Sys SU and Brutsaert DL. Determinants of force decline during relaxation in isolated cardiac muscle. *Am. J. Physiol.* 257:H1490–7, 1989. 2.2, 4.2